The influence of CT and dual-energy X-ray absorptiometry (DXA) bone density on quantitative [18F] sodium fluoride PET

Inderbir S. Jassel[1], Musib Siddique[1], Michelle L. Frost[2]*, Amelia E. B. Moore[2], Tanuj Puri[2], Glen M. Blake[1]

[1]School of Biomedical Engineering & Imaging Sciences, King's College London, St Thomas' Hospital, London, UK; [2]Osteoporosis Research Unit, King's College London, Guy's Hospital, London, UK

Correspondence to: Inderbir S. Jassel. School of Biomedical Engineering & Imaging Sciences, St Thomas' Hospital, London, SE1 7EH, UK. Email: Inderbir.Jassel@nhs.net.

Background: [18F] sodium fluoride PET/CT provides quantitative measures of bone metabolic activity expressed by the parameters standardised uptake value (SUV) and bone plasma clearance (K_i) that correlate with measurements of bone formation rate obtained by bone biopsy with double tetracycline labelling. Both SUV and K_i relate to the tracer uptake in each millilitre of tissue. In general, the bone region of interest (ROI) includes both mineralised bone {generally with a high concentration of [18F]NaF} and bone marrow (with a much lower concentration), suggesting that correcting SUV and K_i for volumetric bone mineral density (vBMD) and measuring them with respect to the tracer uptake in each gram of bone mineral might improve the correlation with the findings of bone biopsy. As a first test of this hypothesis, we looked for positive correlations between SUV and K_i values with CT and DXA bone mineral density (BMD) parameters measured in the same ROI.

Methods: A retrospective reanalysis was performed of 63 lumbar spine [18F]NaF PET/CT scans acquired in four earlier studies. The quantitative PET parameters SUV and K_i were measured in L1–L4 and Hounsfield units (HU) measured on the CT scans in the same ROI. Spine BMD data was also obtained from DXA scans in the form of areal BMD and used to derive the bone mineral apparent density (BMAD, an estimate of vBMD). Scatter plots were drawn of SUV and K_i against HU, BMAD and areal BMD and the Spearman rank correlation coefficients derived for each plot.

Results: All correlations were positive and statistically significant. Correlations were highest for HU (SUV: R_S =0.513, P<0.0001; K_i: R_S =0.429, P=0.0005) and lowest for areal BMD (SUV: R_S =0.353, P=0.005; K_i: R_S =0.274, P=0.03)

Conclusions: The results demonstrate significant positive correlations between SUV and K_i and vBMD measurements in the form of HU from CT or BMAD and areal BMD from DXA. These findings justify further exploration of the relationship between SUV and K_i [18F]NaF PET/CT measurements and CT or DXA measurements of vBMD to examine whether normalization for bone density might improve their correlation with bone metabolic activity as measured by bone biopsy.

Keywords: [18F] sodium fluoride {[18F]NaF}; bone metabolic activity; [18F]NaF bone plasma clearance; computed tomography (CT); dual X-ray absorptiometry (DXA); positron emission tomography (PET); standardised uptake value (SUV)

---

* Present address: Clinical Trials and Statistics Unit, Institute of Cancer Research, Cotswold Road, Sutton, Surrey, SM2 5NG, UK.

Introduction

Positron emission tomography (PET) imaging with fluorine-18-labelled sodium fluoride ([18F]NaF) using hybrid PET and computed tomography (CT) dual-modality (PET/CT) systems is a valuable research tool for examining the quantitative changes in regional bone metabolism that occur in metabolic and metastatic bone disease (1,2). Clinically, [18F]NaF PET/CT imaging is indicated in the identification and assessment of bony metastasis, the evaluation of benign bone disease, in orthopaedic applications and paediatric bone diseases (3).

Bone biopsy with double tetracycline labelling is the gold standard for the direct assessment of bone turnover activity, but is invasive, costly and restricted to the iliac crest (4,5). The cheapest and most widely used method for assessing bone turnover is the measurement of biochemical markers in serum and urine (6,7). However, bone turnover markers provide information on the integrated response across the whole skeleton, and cannot give insight into changes at specific sites such as the spine and hip. Quantitative imaging using [18F]NaF PET/CT provides a unique way of studying bone metabolism that reflects regional bone blood flow and osteoblastic activity and compliments these other methods (8,9).

The simplest method of quantifying [18F]NaF PET/CT studies is to measure standardised uptake values (SUV) by normalising the [18F]NaF concentration in the region of interest (ROI) for injected activity and body weight [SUV = Tissue Activity Concentration (kBq/mL) × Body Weight (kg)/Injected Activity (MBq)] (10). An alternative way of quantifying [18F]NaF PET/CT is the 60-minute dynamic scan method described by Hawkins (11). The bone time-activity curve and the arterial input function are analysed to measure the [18F]NaF plasma clearance to bone mineral (K_i) (units: $mL \cdot min^{-1} \cdot mL^{-1}$). Both SUV and K_i measurements relate to the [18F]NaF activity in each millilitre of tissue and, given the limited spatial resolution of PET images, the bone ROI includes both mineralised bone and bone marrow. However, by the end of a 60-minute [18F]NaF dynamic PET scan the contribution of the tracer uptake in bone mineral to the SUV and K_i measurements is at its highest, while the contribution of tracer in bone marrow has fallen to negligibly low levels. This suggests that correcting SUV and K_i for volumetric bone mineral density (vBMD) obtained by either quantitative CT (QCT) (12) or dual X-ray absorptiometry (DXA) (13), and making measurements that relate to the tracer uptake in each gram of bone mineral instead of each millilitre of volume might improve their correlation with the findings of bone biopsy.

As a first exploration of this hypothesis, we performed a retrospective reanalysis of lumbar spine [18F]NaF PET/CT scans from four previously published studies to measure SUV and K_i in a large number of subjects and study the correlation with Hounsfield units (HU) measurements on CT scans in the same ROI, and bone mineral apparent density (BMAD) (14) and areal BMD measurements from DXA scans in the same vertebrae. A positive correlation between SUV and K_i values with CT and DXA measurements of bone density would justify further exploration of the relationship to examine whether normalization for bone density gives a more accurate representation of bone metabolic activity as measured by bone biopsy.

Methods

Subjects

Lumbar spine [18F]NaF PET/CT scans from four previously published studies (15-18) were recovered from archive for retrospective reanalysis. All the studies were approved by the local ethics committee and the Administration of Radioactive Substances Advisory Committee, and written informed consent was obtained from all participants.

Study 1 consisted of 20 postmenopausal women who at the time of screening had undergone treatment for osteoporosis for at least 3 years with either weekly 70-mg alendronic acid (n=11) or weekly 35-mg risedronate sodium (n=9) (15). Baseline 60-minute dynamic spine [18F]NaF PET/CT scans were performed before bisphosphonate treatment was discontinued, and follow-up scans were performed after 6 and 12 months off therapy. Of the 20 baseline scans, 16 were successfully recovered from archive.

Study 2 consisted of 12 healthy postmenopausal women with no history of metabolic bone disease apart from two with untreated osteoporosis (16). Each subject underwent a 60-minute dynamic [18F]NaF PET/CT scan at the lumbar spine followed two weeks later by a second scan of the proximal femur. Of the 12 spine scans, 9 were recovered from archive.

Study 3 consisted of 27 untreated postmenopausal women with osteopenia who were randomised to either teriparatide with calcium and vitamin D (n=13) or calcium and vitamin D only (n=14) (17). A 60-minute dynamic [18F]NaF PET/CT scan of the hips followed by a 5-minute static

scan of the lumbar spine starting approximately 65 minutes after injection was performed at baseline and after a 12-week treatment. Twenty-five of the twenty-seven baseline spine static PET/CT scans were recovered from archive.

Study 4 consisted of two groups of subjects (18). Study 4A consisted of 12 osteoporotic postmenopausal women, while Study 4B consisted of 7 patients with chronic kidney disease (CKD) (6 M, 1 F). All subjects had a 60-minute dynamic [18F]NaF PET/CT scan of the lumbar spine followed by a 30-minute whole-body scan from skull to mid-femur. Nine of the dynamic spine scans in Study 4A and four from Study 4B were recovered from archive.

[18F]NaF positron emission tomography

All PET/CT scans were acquired using the same GE Discovery PET/CT scanner (General Electric Medical Systems, Waukesha, WI, USA) with a 15.4-cm axial field of view. Where the primary aim was to study the lumbar spine, subjects were injected with 90 MBq [18F]NaF (Studies 1, 2 & 4); where the aim was to study the hip, the dose was doubled to 180 MBq (Study 3). Each 60-minute dynamic scan consisted of 24×5 s, 4×30 s, and 14×240 s frames. Images were reconstructed using filtered back-projection using a 6.3-mm Hanning filter and were corrected for scattered radiation. Low-dose CT scans were performed for attenuation correction. All images were obtained with the subject lying supine and secured with a velcro strap to avoid any movement between the PET and CT scans. The image volume was made up of 47 axial slices. The resolution of each axial slice was 512×512 for CT (with a pixel size of 0.997 mm × 0.997 mm × 3.27 mm in the x, y and z directions) and 128×128 for PET (with a pixel size of 1.664 mm × 1.664 mm × 3.27 mm in the x, y and z directions). Regular quality control and calibration scans were performed on both the PET and CT systems throughout the period of the studies.

During each PET/CT scan, venous blood samples were collected at 30, 40, 50 and 60 minutes after injection—times when arterial and venous concentrations of [18F]NaF in plasma are equal (19). The plasma concentrations at these time points were used to define the terminal exponential up to 60 minutes post injection and the full arterial plasma input function estimated using a semi-population method (20). In this method, a population residual curve, representing the bolus peak and early fast exponentials and derived from the mean curve obtained in ten postmenopausal women by direct arterial sampling (19),

was scaled for injected activity and added to the terminal exponential curve to generate the arterial input function used for kinetic analysis.
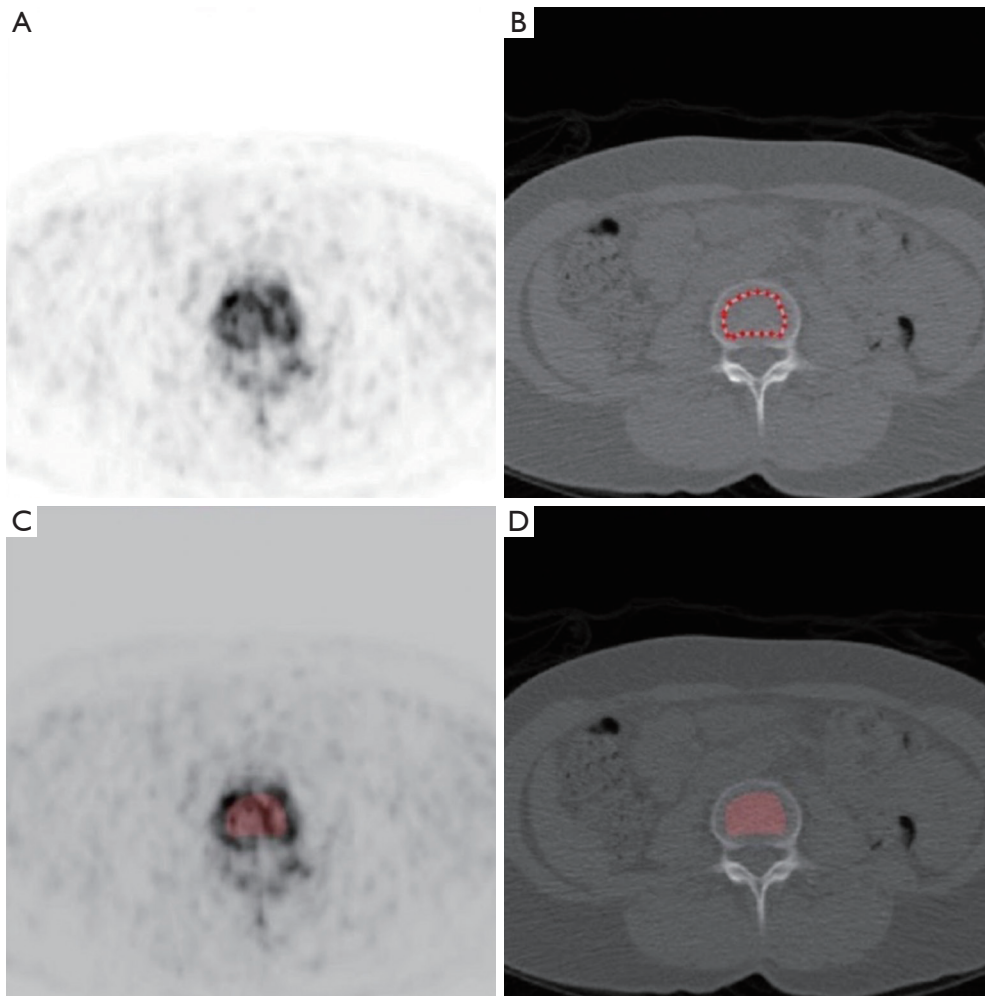
PET scan analysis

The [18F]NaF PET/CT scans were analysed using the static scan method described by Siddique (21,22). In this method, the [18F]NaF bone plasma clearance K_i is estimated from the slope of a Patlak plot constructed from just two data points: the first point is obtained from the regional [18F]NaF activity concentration measured in a single static scan acquired between 45 and 75 minutes after injection, and the second point is derived from the average value of the intercept of the Patlak plot obtained in a study of 36 postmenopausal women (22). In the present study, the static scan was generated from either the final 240-s frame of the 60-minute dynamic spine scan (Studies 1, 2 & 4) or the static scan of the spine acquired 65 minutes after injection (Study 3).

Figure 1 shows representative images illustrating our method of scan analysis. For each axial CT slice of the L1–L4 lumbar vertebrae a ROI was set manually within the central trabecular region taking care to avoid the surrounding cortical bone and an identical ROI automatically overlaid on the corresponding PET image. For the PET scans, there were typically four axial slices available within each vertebral body after the endplates were excluded. Static scan K_i values were calculated using Siddique's method assuming a Patlak plot intercept of 0.22 and a mean rate constant for the efflux of [18F]NaF tracer from bone of 0.006 min^{-1} (22). SUVs were calculated from the mean concentration of [18F]NaF activity in the bone ROI. Mean values of K_i and SUV were calculated within each PET ROI and mean HU within the corresponding CT ROI. The K_i, SUV and HU values for the four vertebral body ROIs within each PET/CT scan field of view were averaged to generate a single lumbar spine K_i, SUV and HU result for each scan.

Measurements of bone mineral density (BMD)

Lumbar spine DXA scans (L1–L4) were performed in all four studies (Hologic Discovery; Hologic Inc., Marlborough, MA) and used to measure the areal BMD and bone mineral content (BMC). The total projected area of the L1–L4 vertebrae was divided by the length of the vertebral column between the T12/L1 and L4/L5 disc spaces to calculate the mean width of the L1–L4 lumbar

Figure 1 Representative images illustrating the method of scan analysis. (A,B) Matching [^{18}F]NaF PET and CT images showing the placement of the region of interest (ROI) within trabecular bone in a lumbar vertebra using the CT image; (C,D) the red shaded areas show the ROI in (B) superimposed on the PET and CT images.

vertebrae. Bone mineral apparent density (BMAD), an estimate of the mean volumetric BMD of the lumbar spine, was calculated by dividing the BMC of the L1–L4 vertebrae by their estimated volume on the assumption that the vertebral column has cylindrical geometry (14).

HU measurements from the CT scans acquired for attenuation correction of the PET scans and obtained in the same ROI used for the SUV and K_i analysis were used as an estimate of volumetric BMD in trabecular bone in the lumbar vertebral bodies and averaged over the L1–L4 vertebrae.

Statistical analysis

Scatter plots were drawn of K_i and SUV values for each subject plotted against the CT-HU measurements and the DXA-BMAD and areal BMD measurements. The statistical significance of each relationship was evaluated using Spearman's rank correlation test. A two-tailed P value <0.05 was taken to be statistically significant.

Results

At total of 63 [^{18}F]NaF PET/CT scans from the four studies were recovered from archive. One subject from Study 3 had degenerative disease in the lumbar spine affecting her DXA scan results and was excluded, leaving a total of 62 subjects for statistical analysis. Full demographic details for each study were published previously (15-18). Results of
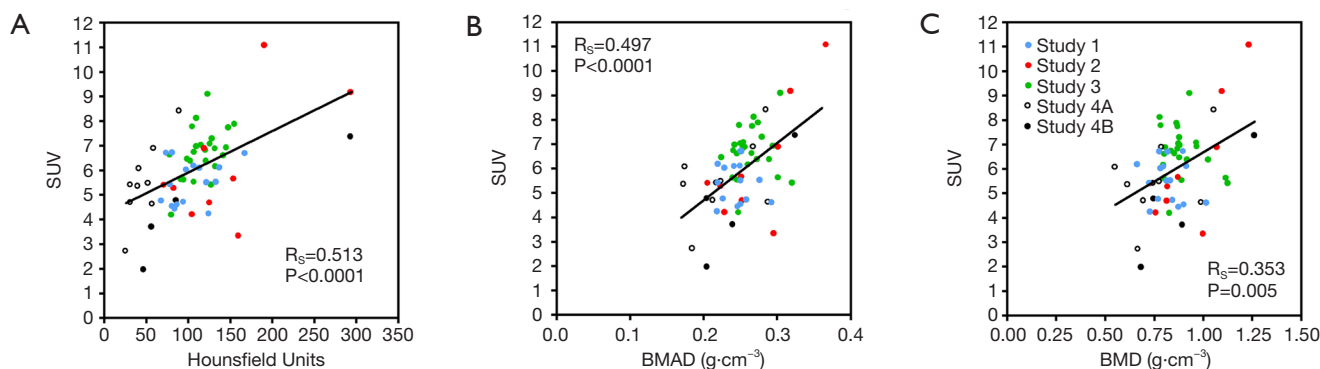
Figure 2 Scatter plots showing the relationship between mean standardised uptake value (SUV) in the lumbar spine and (A) Hounsfield units, (B) bone mineral apparent density (BMAD), and (C) areal bone mineral density (BMD). R_S, Spearman rank correlation coefficient.
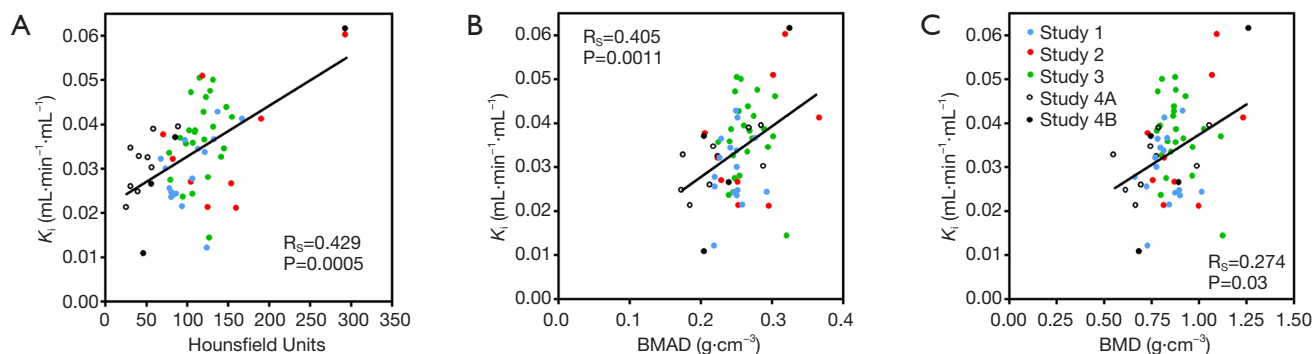
Figure 3 Scatter plots showing the relationship between mean [18F]NaF bone plasma clearance to the lumbar spine (K_i) and (A) Hounsfield units, (B) bone mineral apparent density (BMAD), and (C) areal bone mineral density (BMD). R_S, Spearman rank correlation coefficient.

the Spearman rank correlation tests when SUV was plotted against HU, BMAD and BMD, ranged from R_S =0.513 (P<0.0001) to R_S =0.353 (P=0.005) (*Figure 2*). The results when K_i was plotted against HU, BMAD and BMD ranged from R_S =0.429 (P=0.0005) to R_S =0.274 (P=0.03) (*Figure 3*).

Discussion

The results of this study confirm our prediction of correlations between the [18F]NaF PET volumetric parameters SUV and K_i measured in vertebral trabecular bone and bone density measurements in the same vertebrae made using CT and DXA. *Figure 2* demonstrates significant positive correlations between the mean SUV measured in the L1–L4 lumbar vertebrae and the three different measures of bone density. The correlation was strongest for the CT-HU measurements, and weakest for the DXA measurements of areal BMD. These findings are in keeping with results reported by Cachovan *et al.* (23) which

demonstrated a statistically significant correlation (r=0.678, P<0.0001, n=50) between lumbar vertebra measurements of SUV obtained in [99mTc]TcDPD SPECT/CT images and the HU measurements obtained from the associated CT scans. Although a direct comparison cannot be made due to the different modality and radiotracer used to derive SUV, the bone imaging tracers, [99mTc]TcDPD and [18F]NaF, bind to sites of newly mineralising bone by similar mechanisms.

Figure 3 shows similar correlations between the Hawkins model's bone metabolic parameter K_i and the same three bone density parameters, with the correlations again being strongest for HU and weakest for DXA areal BMD. This is in contrast to the results of measurements in adult female mini pigs reported by Piert *et al.* (8) in which no significant correlation was found between CT measurements of volumetric BMD calibrated with a hydroxyapatite phantom and averaged over cortical and trabecular bone, and K_i measured with [18F]NaF PET. This difference in results could be due to the small number of mini pigs in the

206

Jassel et al. Bone density and [^{18}F] uoride PET

BMD study (n=5), or to the inclusion of both cortical and trabecular bone in the CT measurements. In the present study, the HU measurements were made exclusively in trabecular bone.

In both *Figures 2* and *3* the Spearman correlation coefficient between the PET parameters and BMAD is intermediate in value between those for HU and DXA-BMD. A DXA scan is a two-dimensional (2D) projection scan that measures areal BMD in units of g/cm^2 and provides no information about bone thickness in the anteroposterior direction. BMAD provides an estimate of volumetric bone density (units: g/cm^3) on the assumption that the missing measurement of bone thickness is highly correlated with the width of bone on the 2D DXA scan. It therefore provides information that is intermediate between DXA areal BMD and a QCT measurement of true volumetric BMD, but its reliability is dependent on the degree of correlation between bone thickness and bone width.

It is conventional to interpret measurements of [^{18}F]NaF bone plasma clearance and SUV in the skeleton as indicators of bone metabolic activity (8,24). Although the correlation coefficients in *Figures 2* and *3* are weak, the present investigation demonstrates that measurements of BMD by QCT or DXA are significant covariates of SUV and K_i that should be taken into account in future studies. The present study included all the subjects for whom PET/CT scan data were available and were individuals with a variety of bone turnover states. Subjects in Study 1 were postmenopausal women on long-term antiresorptive therapy for osteoporosis in whom bone turnover was suppressed (25,26). Consistent with this, a study of the effect of 6-month treatment with risedronate on quantitative [^{18}F]NaF PET showed an 18% decrease in lumbar spine K_i (27).

Subjects in studies 2, 3 and 4A were untreated postmenopausal women expected to have raised bone turnover compared with premenopausal women (5,28,29). A [^{18}F]NaF PET study in untreated postmenopausal women found a statistically significant increase in levels of the bone formation marker serum bone specific alkaline phosphatase in subjects with osteoporosis compared with those with a normal DXA T-score (30). Although measurements of lumbar spine K_i were statistically significantly lower by 17% in the osteoporotic women compared with those with normal T-scores, after correction for DXA-BMD, the results for osteoporotic women were statistically significantly higher by 21% than those in women with normal T-scores. This finding is consistent with the conclusions of the present study which indicate that

bone density measurements have a significant role in the interpretation of quantitative [^{18}F]NaF PET measurements of bone metabolic activity.

Subjects in Study 4B were patients with CKD Stage 5 on haemodialysis (18). Renal osteodystrophy is a complex condition with a spectrum of bone turnover states that are difficult to differentiate without a bone biopsy, and range from adynamic bone disease, where bone turnover is greatly reduced, to high turnover bone disease, due to the development of secondary hyperparathyroidism (24,31).

Although it is plausible to anticipate a correlation between quantitative parameters of [^{18}F]NaF uptake in bone and measurements of volumetric BMD, it is unclear whether bone density is the optimum parameter for the purpose of normalizing SUV and K_i to the amount of bone present in each millilitre of tissue. Within vertebral bodies, the trabecular bone presents a vast surface area on which the processes of bone remodelling are continually occurring. In the analysis of bone biopsy samples with double tetracycline labelling, measurements are made of the surface area of trabeculae, the area of actively mineralising surface, and the mineral apposition rate, so that bone formation rate is normalised to the total area of bone surface. There is therefore a rationale for believing that normalising SUV and K_i to the surface area of trabeculae within the PET ROI might be the most appropriate method of expressing the bone metabolic activity in each millilitre of tissue. However, given the absence of a practical method of measuring bone trabecular surface area in the spine, BMD is the most suitable substitute.

This study has a number of limitations. A comprehensive study of the correlations between [^{18}F]NaF SUV and K_i measurements and BMD would require a bone biopsy in every subject to verify the association with bone metabolic activity. The ROIs were drawn manually by a user who visually identified the trabecular regions of the L1–L4 lumbar vertebrae on the [^{18}F]NaF PET/CT scans (*Figure 1B*). This process is subject to human error, and could have been improved using techniques such as greyscale thresholding to differentiate between cortical and trabecular bone. The PET scans were reconstructed using filtered back-projection rather than an iterative algorithm, as this was the advice we received at the time the original investigations were performed (15-18). At the time the PET/CT scans were performed, no phantom was available to calibrate the HU measurements and convert them into measurements of volumetric BMD. In QCT, it is usual to scan each subject with a phantom which contains

standards with known densities of hydroxyapatite to derive a linear calibration plot between HU and volumetric BMD. Recently, asynchronous QCT has been developed which does not require the presence of a phantom during scanning, but enables CT scans to be retrospectively calibrated to measure volumetric BMD by providing a single calibration curve that is applied to all previous scans (32). Asynchronous QCT is recommended for quantifying BMD for PET/CT studies as it avoids the complication of having to acquire the PET images in the presence of a calibration phantom. Had asynchronous QCT been available for the present study, then the only thing that would change in *Figures 2A* and *3A* would be a rescaling of the data points on the horizontal axis. The order of ranking of the data, and thus the Spearman correlation coefficient and its statistical significance, would be unchanged. Hence, the absence of a calibration curve to convert HU into volumetric BMD does not change the statistical significance of the results reported here. Finally, the data presented here were derived by pooling [^{18}F]NaF PET/CT scans from a number of separate studies to obtain the largest available set of results for statistical analysis. [^{18}F]NaF PET and the associated CT scans were recovered from archive for 63 out of the total of 78 subjects potentially available (80%). Although this is a heterogeneous group of subjects, there is a trend for SUV and K_i to correlate positively with bone density in the majority of the separate studies plotted in *Figures 2* and *3*. The exception is the areal BMD plots for Studies 1 and 3 in *Figures 2C* and *3C*, where the range of areal BMD values was narrowed by their restriction to osteoporotic and osteopenic subjects defined according to their DXA T-scores.

Conclusions

The results of this study demonstrate that [^{18}F]NaF PET/CT measurements of lumbar spine SUV and the Hawkins' model bone metabolic parameter K_i correlate with CT measurements of HU and DXA measurements of BMAD and areal BMD. This suggests that normalization of PET volumetric measures of bone tracer uptake and bone plasma clearance to the mass of mineralised bone present in each millilitre of tissue might correlate better with the gold standard of bone biopsy and therefore may be a more appropriate way of expressing bone metabolic activity than the conventional normalization to tissue volume. The study further shows that bone density measurements obtained by QCT or DXA are a significant covariate of quantitative

radionuclide measurements of bone metabolic activity that should be considered when analysing the results of future studies. These results justify further studies to examine the effect of combining PET and bone density measurements when assessing bone metabolism in comparison to the gold standard of bone biopsy.

Footnote

Conflicts of Interest: The authors have no conflicts of interest to declare.

Ethical Statement: All the studies were approved by the local ethics committee and the Administration of Radioactive Substances Advisory Committee, and written informed consent was obtained from all participants.

References

1. Raynor W, Houshmand S, Gholami S, Emamzadehfard S, Rajapakse CS, Blomberg BA, Werner TJ, Høilund-Carlsen PF, Baker JF, Alavi A. Evolving Role of Molecular Imaging with ^{18}F-Sodium Fluoride PET as a Biomarker for Calcium Metabolism. Curr Osteoporos Rep 2016;14:115-25.
2. Blake GM, Puri T, Siddique M, Frost ML, Moore AEB, Fogelman I. Site specific measurements of bone formation using [^{18}F] sodium fluoride PET/CT. Quant Imaging Med Surg 2018;8:47-59.
3. Beheshti M, Mottaghy FM, Paycha F, Behrendt FFF, Van den Wyngaert T, Fogelman I, Strobel K, Celli M, Fanti S, Giammarile F, Krause B, Langsteger W. (18)F-NaF PET/CT: EANM procedure guidelines for bone imaging. Eur J Nucl Med Mol Imaging 2015;42:1767-77.
4. Dempster DW, Zhou H, Recker RR, Brown JP, Recknor

CP, Lewiecki EM, Miller PD, Rao SD, Kendler DL, Lindsay R, Krege JH, Alam J, Taylor KA, Melby TE, Ruff VA. Remodeling- and Modeling-Based Bone Formation With Teriparatide Versus Denosumab: A Longitudinal Analysis From Baseline to 3 Months in the AVA Study. J Bone Miner Res 2018;33:298-306.

5. Recker RR, Lappe JM, Davies M, Kimmel D. Perimenopausal bone histomorphometry before and after menopause. Bone 2018;108:55-61.

6. Eastell R, Szulc P. Use of bone turnover markers in postmenopausal osteoporosis. Lancet Diabetes Endocrinol 2017;5:908-923.

7. Glover SJ, Gall M, Schoenborn-Kellenberger O, Wagener M, Garnero P, Boonen S, Cauley JA, Black DM, Delmas PD, Eastell R. Establishing a reference interval for bone turnover markers in 637 healthy, young, premenopausal women from the United Kingdom, France, Belgium, and the United States. J Bone Miner Res 2009;24:389-97.

8. Piert M, Zittel TT, Becker GA, Jahn M, Stahlschmidt A, Maier G, Machulla HJ, Bares R. Assessment of porcine bone metabolism by dynamic ¹⁸F-fluoride PET: correlation with bone histomorphometry. J Nucl Med 2001;42:1091-100.

9. Czernin J, Satyamurthy N, Schiepers C. Molecular mechanisms of bone ¹⁸F-NaF deposition. J Nucl Med 2010;51:1826-9.

10. Sabbah N, Jackson T, Mosci C, Jamali M, Minamimoto R, Quon A, Mittra ES, Iagaru A. ¹⁸F-sodium fluoride PET/CT in oncology: an atlas of SUVs. Clin Nucl Med 2015;40:e228-31.

11. Hawkins RA, Choi Y, Huang SC, Hoh CK, Dahlbom M, Schiepers C, Satyamurthy N, Barrio JR, Phelps ME. Evaluation of the skeletal kinetics of fluorine-18-fluoride ion with PET. J Nucl Med 1992;33:633-42.

12. Engelke K, Adams JE, Armbrecht G, Augat P, Bogado CE, Bouxsein ML, Felsenberg D, Ito M, Prevrhal S, Hans DB, Lewiecki EM. Clinical use of quantitative computed tomography and peripheral quantitative computed tomography in the management of osteoporosis in adults: the 2007 ISCD Official Positions. J Clin Densitom 2008;11:123-62.

13. Malabanan AO, Rosen HN, Vokes TJ, Deal CL, Alele JD, Olenginski TP, Schousboe JT. Indications of DXA in women younger than 65 yr and men younger than 70 yr: the 2013 Official Positions. J Clin Densitom 2013;16:467-71.

14. Carter DR, Bouxsein ML, Marcus R. New approaches for interpreting projected bone densitometry data. J Bone

Miner Res 1992;7:137-45.

15. Frost ML, Siddique M, Blake GM, Moore AE, Marsden PK, Schleyer PJ, Eastell R, Fogelman I. Regional bone metabolism at the lumbar spine and hip following discontinuation of alendronate and risedronate treatment in postmenopausal women. Osteoporos Int 2012;23:2107-16.

16. Puri T, Frost ML, Curran KM, Siddique M, Moore AE, Cook GJ, Marsden PK, Fogelman I, Blake GM. Differences in regional bone metabolism at the spine and hip: a quantitative study using ¹⁸F-fluoride positron emission tomography. Osteoporos Int 2013;24:633-9.

17. Frost ML, Moore AE, Siddique M, Blake GM, Laurent D, Borah B, Schramm U, Valentin MA, Pellas TC, Marsden PK, Schleyer PJ, Fogelman I. 18F-fluoride PET as a noninvasive imaging biomarker for determining treatment efficacy of bone active agents at the hip: a prospective, randomized, controlled clinical study. J Bone Miner Res 2013;28:1337-47.

18. Frost ML, Compston JE, Goldsmith D, Moore AE, Blake GM, Siddique M, Skingle L, Fogelman I. ¹⁸F-fluoride positron emission tomography measurements of regional bone formation in hemodialysis patients with suspected adynamic bone disease. Calcif Tissue Int 2013;93:436-47.

19. Cook GJ, Lodge MA, Marsden PK, Dynes A, Fogelman I. Non-invasive assessment of skeletal kinetics using fluorine-18 fluoride positron emission tomography: evaluation of image and population-derived arterial input functions. Eur J Nucl Med 1999;26:1424-9.

20. Blake GM, Siddique M, Puri T, Frost ML, Moore AE, Cook GJ, Fogelman I. A semipopulation input function for quantifying static and dynamic ¹⁸F-fluoride PET scans. Nucl Med Commun 2012;33:881-8.

21. Siddique M, Blake GM, Frost ML, Moore AE, Puri T, Marsden PK, Fogelman I. Estimation of regional bone metabolism from whole-body ¹⁸F-fluoride PET static images. Eur J Nucl Med Mol Imaging 2012;39:337-43.

22. Siddique M, Frost ML, Moore AE, Fogelman I, Blake GM. Correcting ¹⁸F-fluoride PET static scan measurements of skeletal plasma clearance for tracer efflux from bone. Nucl Med Commun 2014;35:303-10.

23. Cachovan M, Vija AH, Hornegger J, Kuwert T. Quantification of ⁹⁹ᵐTc-DPD concentration in the lumbar spine with SPECT/CT. EJNMMI Res 2013;3:45.

24. Messa C, Goodman WG, Hoh CK, Choi Y, Nissenson AR, Salusky IB, Phelps ME, Hawkins RA. Bone metabolic activity measured with positron emission tomography and [¹⁸F]fluoride ion in renal osteodystrophy: correlation

with bone histomorphometry. J Clin Endocrinol Metab 1993;77:949-55.

25. Garnero P, Shih WJ, Gineyts E, Karpf DB, Delmas PD. Comparison of new biochemical markers of bone turnover in late postmenopausal osteoporotic women in response to alendronate treatment. J Clin Endocrinol Metab 1994;79:1693-700.

26. Dufresne TE, Chmielewski PA, Manhart MD, Johnson TD, Borah B. Risedronate preserves bone architecture in early postmenopausal women in 1 year as measured by three-dimensional microcomputed tomography. Calcif Tissue Int 2003;73:423-32.

27. Frost ML, Cook GJ, Blake GM, Marsden PK, Benatar NA, Fogelman I. A prospective study of risedronate on regional bone metabolism and blood flow at the lumbar spine measured by 18F-fluoride positron emission tomography. J Bone Miner Res 2003;18:2215-22.

28. Garnero P, Sornay-Rendu E, Chapuy MC, Delmas PD. Increased bone turnover in late postmenopausal women

is a major determinant of osteoporosis. J Bone Miner Res 1996;11:337-49.

29. Recker R, Lappe J, Davies KM, Heaney R. Bone remodeling increases substantially in the years after menopause and remains increased in older osteoporosis patients. J Bone Miner Res 2004;19:1628-33.

30. Frost ML, Fogelman I, Blake GM, Marsden PK, Cook GJR. Dissociation between global markers of bone formation and direct measurement of spinal bone formation in osteoporosis. J Bone Miner Res 2004;19:1797-804.

31. Martin KJ, González EA. Metabolic bone disease in chronic kidney disease. J Am Soc Nephrol 2007;18:875-85.

32. Wang L, Su Y, Wang Q, Duanmu Y, Yang M, Yi C, Cheng X. Validation of asynchronous quantitative bone densitometry of the spine: Accuracy, short-term reproducibility, and a comparison with conventional quantitative computed tomography. Sci Rep 2017;7:6284.